Low-Bias Control of AMB's Subject to Saturation Constraints

Panagiotis Tsiotras and Efstathios Velenis
School of Aerospace Engineering
Georgia Institute of Technology, Atlanta, GA 30332-0150, USA
p.tsiotras@ae.gatech.edu, gte600q@prism.gatech.edu

Abstract

This paper addresses the problem of low-bias control for an active magnetic bearing (AMB). Using a complementarity flux condition, a simplified, three-dimensional model is used to describe the dynamics of this mode of operation. Recent results from the theory of saturating control are used to design a stabilizing controller. The saturation level is a free parameter that is chosen by the control engineer. Numerical simulations at the end of the paper show the effectiveness of the design method proposed.

1 Introduction

It is envisioned that future commercial and military spacecraft will have an unprecedented degree of autonomy made possible by increased on-board processing speed and memory capabilities. This increase in on-board processing, autonomous sensing and communication capabilities translates directly to large requirements in on-board available power. Traditional chemical batteries have several limitations stemming from their inherent unreliability, low depth of discharge, heavy weight, limited life, etc. A discussion on the future trends of satellite architectures and their impact on power generation and storage requirements can be found in [13, 4, 16].

An alternative to the chemical batteries for energy storage and power generation for future spacecraft has been proposed in recent years, namely, that of electromechanical (e.g., flywheel) batteries [2, 3, 7, 13, 15]. Taking into consideration that most orbiting spacecraft already incorporate moving wheels (e.g., reaction, momentum wheels, CMG's) for attitude control, the prospect of using these spinning wheels to also store energy seems natural and appealing. Several technical challenges need to be overcome, however, before efficient flywheels become a part of a standard spacecraft power subsystem. One such major challenge is the design of low-loss flywheels supported on active magnetic bearings (AMB's).

Efficiency of flywheel operation implies low losses (mechanical and other). To avoid excessive friction losses, the use of AMB's to support the spinning rotor is thus inevitable. A major source of power loss in a flywheel/AMB system is due to eddy current effects. These losses can be a significant portion of the overall power losses in high-speed flywheels [1]. One way to reduce eddy current losses is to reduce or eliminate the bias current during AMB operation [8, 9]. Since the flux/force characteristic of an AMB is nonlinear, bias flux (or current) is typically used to linearize the AMB about an operating point. Reduction of the bias current leads to the nonlinear region which is dominated, among other things, by slew-rate force limitations close to the origin [5]. These limitations manifest themselves, in effect, as power amplifier voltage saturation. The problem of designing low-bias control laws for AMB's subject to control saturation constraints is a therefore a nontrivial nonlinear problem.

In this paper we use the recent results from the theory of saturating control in order to design stabilizing control laws for AMBs in low bias operation, subject to saturation constraints. The main design tool in this framework is an asymptotic small-gain theorem due to Teel [19]. Additional results for saturating control design for linear and nonlinear systems can be found in [11, 17, 18]. We present two low-bias designs. The first design ensures global asymptotic stability in case of a soft saturation constraint. The second design ensures local asymptotic stability for a hard saturation constraint. Both designs allow one to choose the saturation level accordingly.

2 Modeling of an AMB in Low Bias Mode

The simplified AMB model used in this paper consists of two identical electromagnets, used to move a mass m in one dimension. To regulate the position x of the mass to zero, the control designer uses the voltage inputs of the electromagnets, e_1 and e_2, in order to vary the forces acting on the rotor; see Fig. 1.

The total force generated by each electromagnet is given by [14]

$$F_i = \frac{\Phi_i^2}{\mu_o A_g}, \qquad i = 1, 2 \tag{1}$$

where Φ_i is the total magnetic flux of the i-th electromagnet, A_g is the cross sectional area of airgap and μ_o is the permeability of free space ($= 1.25 \times 10^{-6}\ H/m$). In bias operation we distinguish the total magnetic flux into the bias flux Φ_o, which is the minimum amount of flux produced by each electromagnet separately at all times, and the perturbation (control) flux $\Delta\Phi_i$ produced by the i-th electromagnet. The total flux generated by the i-th electromagnet is

$$\Phi_i = \Phi_o + \Delta\Phi_i, \qquad i = 1, 2 \tag{2}$$

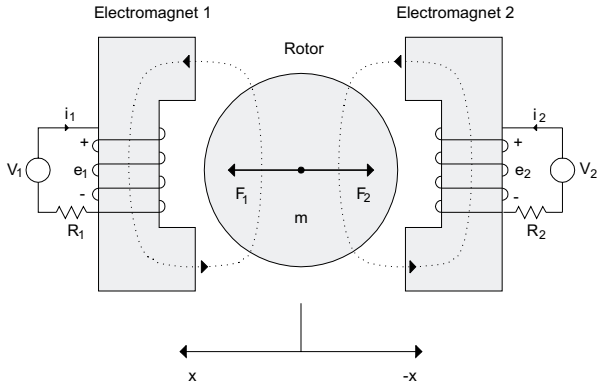

Figure 1: Simplified AMB model.

The equation of motion of the rotor about an axis perpendicular to the axis of rotation, not taking into account the gravity, can be written as

$$\begin{aligned} \ddot{x} &= \frac{1}{k}(\Phi_1^2 - \Phi_2^2) \\ &= \frac{1}{k}\left[\Delta\Phi_1^2 - \Delta\Phi_2^2 + 2\Phi_o(\Delta\Phi_1 - \Delta\Phi_2)\right] \quad (3) \end{aligned}$$

where $k = m\mu_o A_g$. The complementary flux condition requires the control flux to be generated by only one of the electromagnets at a time, depending on the direction of the force we need to apply. Thus,

$$\Delta\Phi_1 = \Delta\Phi,\ \Delta\Phi_2 = 0 \qquad \text{when} \quad \Delta\Phi \geq 0 \quad (4a)$$
$$-\Delta\Phi_2 = \Delta\Phi,\ \Delta\Phi_1 = 0 \qquad \text{when} \quad \Delta\Phi \leq 0 \quad (4b)$$

The dynamics of the system can be rewritten as

$$\ddot{x} = \frac{1}{k}\left(\Delta\Phi\,|\Delta\Phi| + 2\Phi_o\Delta\Phi\right) \quad (5)$$

Defining the state and control variables $x_1 = kx$, $x_2 = k\dot{x}$, $x_3 = \Delta\Phi$, $v = \Delta\dot{\Phi}$, system can be written in the following state space form:

$$\begin{aligned} \dot{x}_1 &= x_2 \\ \dot{x}_2 &= \varepsilon x_3 + x_3\,|x_3| \quad (6) \\ \dot{x}_3 &= v \end{aligned}$$

where $\varepsilon = 2\Phi_o$. In this model ε is a small parameter representing the bias flux applied. Notice that for $\varepsilon = 0$ the model reduces to the zero bias case.
In formulating the above equations we have assumed negligible coil resistance, such that

$$v = \Delta\dot{\Phi} = \frac{\Delta e}{N} \quad (7)$$

where N is the number of turns of the coil of each electromagnet and Δe is the control voltage applied to each electromagnet. In reality, the last equation in (6) should be substituted by $\dot{x}_3 = \text{sat}(v)$ to enforces the constraint on the maximum voltage allowed. Without loss of generality, in the sequel we take the saturation level to be unity.

3 Low-bias vs. Zero-bias AMB Operation

The main reason for low-bias operation is, as stated above, the reduction of power loses. In addition to using low bias, the complementary flux condition (4) is also used, so as not to apply control fluxes (and hence forces) that oppose each other. In the limiting case, zero-bias control (along with the complementary flux condition) can be used to eliminate completely any opposing fluxes during AMB operation. Zero-bias operation however imposes severe limitations on the AMB operation. Thus, typically a low-bias operation is used in practice. The difficulties arising for zero-bias operation become apparent when looking at the plot of applied flux vs. total generated force for each mode, shown in Fig. 2.

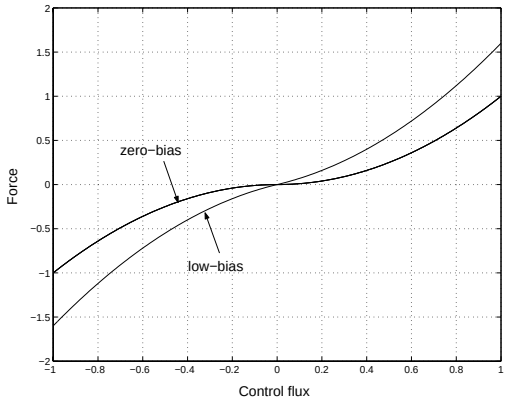

Figure 2: Zero-bias and Low-bias characteristics.

For low-bias operation, the relation between the applied control flux $\Delta\Phi$ and the total generated force on the rotor is given by (5). From Eq. (5), setting $\Phi_o = 0$ we obtain the dynamics of an AMB for zero-bias operation

$$\ddot{x} = \frac{1}{k}\,\Delta\Phi\,|\Delta\Phi| = \frac{1}{k}\,\Phi\,|\Phi| \quad (8)$$

From Fig. 2 it is seen that for the zero-bias case the slope near the origin is zero. This implies that in order to produce a small control force we need a large change in flux. In other words, for zero-bias operation, we have a situation resembling a 'dead zone' near the origin. This problem is eliminated using bias operation. Note that as the bias flux increases the slope at the origin gets steeper, leading to better dynamic response of the AMB. This is achieved at a price of higher power losses. A compromise is need between the slope at the origin and the power losses due to bias fluxes. This compromise leads us to the low bias control design presented in this paper.

4 Asymptotic Small Gain Theorem

In this section we present the main theoretical result used in this paper to solve the stabilization problem

in Eq. (6). This results is the asymptotic small gain theorem by Teel [19]. It provides us with stability conditions for interconnected systems, whose norms of the output satisfy certain asymptotic bounds. Before presenting the main result from [19] used in this paper we need to introduce some preliminary notation.
Let $|y| := \max_i |y_i|$ denote the norm for a vector $y \in \Re^n$. For a signal y let

$$\|y\|_a = \lim_{t\to\infty} \sup |y(t)| \tag{9}$$

We will say that the signal y satisfies an asymptotic bound δ if $\|y\|_a \leq \delta$.
Consider the interconnection of two systems P_1, P_2 with inputs u_1, u_2, outputs y_1, y_2 and disturbances d_1, d_2, respectively. Let δ_1 and δ_2 denote known asymptotic bounds of the disturbances d_1 and d_2, i.e, $\|d_i\|_a \leq \delta_i$, for $i = 1, 2$.

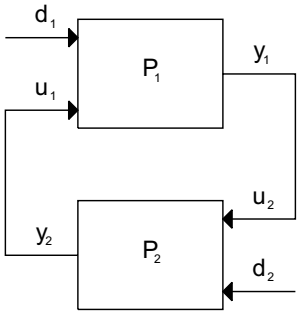

Figure 3: System interconnection.

We assume that the systems P_1 and P_2 satisfy the following conditions

$$(P_1): \quad \|y_2\|_a \leq \Delta \Rightarrow \|y_1\|_a \leq \max\{\gamma_1(\|y_2\|_a), \delta_1\} \tag{10}$$
$$(P_2): \quad \|y_2\|_a \leq \max\{\gamma_2(\|y_1\|_a), \delta_2\} \tag{11}$$

where γ_1 and γ_2 are the asymptotic gains of the two systems. That is, $\gamma_i : \Re_+ \to \Re_+$, $i = 1, 2$ are nondecreasing continuous functions with $\gamma_i(0) = 0$. Qualitatively, conditions (10) and (11) imply a *weak interconnection* of the two systems. The worst case asymptotic behavior of P_1 has a limited impact on the worst case asymptotic behavior of P_2. For such a system interconnection Teel [19] proposed the so-called asymptotic small gain theorem.

Theorem 1 ([19],[6]) *Let P_1 and P_2 be two systems satisfying the weak interconnection conditions (10) and (11). Assume the interconnection is well-posed and there are no finite escape times. Assume that*

$$(i) \quad \gamma_1(\gamma_2(s)) < s, \quad \forall s > 0 \tag{12}$$
$$(ii) \quad \max\{\gamma_2(\infty), \delta_2\} \leq \Delta < \infty \tag{13}$$

where $\gamma_2(\infty) = \lim_{s\to\infty} \gamma_2(s)$. Then

$$\|y_1\|_a \leq \max\{\gamma_1(\delta_2), \delta_1\} \tag{14}$$
$$\|y_2\|_a \leq \max\{\gamma_2(\delta_1), \delta_2\} \tag{15}$$

Notice that when $d_2 = 0$ then $\|y_2\|_a \leq \gamma_2(\delta_1)$ and $\|y_1\|_a \leq \delta_1$. Moreover, if $\delta_1 = 0$ (i.e, the system P_1 is driven by an asymptotically vanishing disturbance) then y_1 and y_2 converge to zero. In particular, if the outputs are the states of the two systems, asymptotic stability follows immediately[1].

5 Application to the Low-bias AMB

To apply the previous design methodology to the AMB low-bias problem, first we use the preliminary feedback

$$v = -k_2 x_2 - k_3 x_3 + u \tag{16}$$

such that the closed loop system (6) takes the form

$$\dot{x} = Ax + Bu + d \tag{17}$$

where

$$A = \begin{bmatrix} 0 & 1 & 0 \\ 0 & 0 & \varepsilon \\ 0 & -k_2 & -k_3 \end{bmatrix}, \; B = \begin{bmatrix} 0 \\ 0 \\ 1 \end{bmatrix}, \; d = \begin{bmatrix} 0 \\ x_3\,|x_3| \\ 0 \end{bmatrix} \tag{18}$$

where k_2 and k_3 are positive scalars such that the matrix A is neutrally stable, i.e., there exists a positive definite matrix $P > 0$ such that $A^T P + PA \leq 0$. Next, re-write (18) as a feedback interconnection of the following two systems (see also Fig. 4)

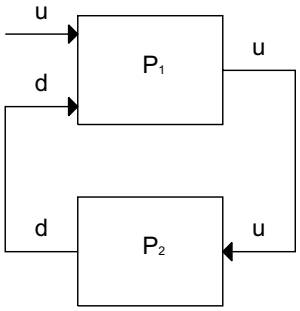

Figure 4: System decomposition for the AMB problem.

$$(P_1): \quad \begin{array}{l} \dot{x} = Ax + Bu + d \\ y_1 = u \end{array} \tag{19}$$

and

$$(P_2): \quad \begin{array}{l} \dot{x}_2 = \varepsilon x_3 + x_3\,|x_3| \\ \dot{x}_3 = -k_2 x_2 - k_3 x_3 + u \\ y_2 = x_3 |x_3| \end{array} \tag{20}$$

Note that the system P_1 outputs its own input u, while the system P_2 has only one input u and outputs the disturbance $d = x_3|x_3|$ for the system P_1.
In order to apply Theorem 1 to the system interconnection (19)-(20) we make use of the following two lemmas.

[1] Strictly speaking, we have shown only convergence of the states to the origin. Stability can be shown by examining the linearization of the interconnection around the origin.

Lemma 1 *Let the system (20). There exist positive numbers b_i (i=1,...,4) such that*

$$\|x_3\|_a \leq \gamma_2'(\|u\|_a) \tag{21}$$

where $\gamma_2'(s) = \sqrt{b_1 s^2 + b_2 s^3 + (b_3 s^2 + b_4 s^3)^{3/2}}$.

Proof: Let the function $V : \Re^3 \to \Re_+$ defined by

$$V = \frac{k_2}{2}x_2^2 + \frac{\varepsilon}{2}x_3^2 + \mu x_2 x_3 + \frac{1}{3}|x_3|x_3^2 \tag{22}$$

where

$$0 < \mu < \min\{k_3, \sqrt{k_2\varepsilon}, \frac{4\varepsilon k_2 k_3}{4\varepsilon k_2 + k_3^2}\} \tag{23}$$

It can be readily shown that V is positive definite. Taking now the derivative of V along the trajectories of (20) one obtains

$$\begin{aligned}\dot{V} &= -\varepsilon\bar{\mu}x_3^2 - k_2\mu x_2^2 - \mu k_3 x_2 x_3 \\ &\quad -\bar{\mu}|x_3|x_3^2 + \varepsilon x_3 u + u|x_3|x_3 + \mu x_2 u \\ &\leq -a_1|x|^2 + (\varepsilon+\mu)|x||u| + |u||x_3|^2 - \bar{\mu}|x_3|^3\end{aligned}$$

where

$$a_1 = \left(\varepsilon\bar{\mu} + \mu k_2 - \sqrt{(\varepsilon\bar{\mu} - \mu k_2)^2 + \mu^2 k_3^2}\right)/2$$

and $\bar{\mu} = k_3 - \mu$. Notice that $a_1 > 0$ by (23). Using Young's inequality [10, p.75] we have

$$|u||x_3|^2 \leq \frac{4}{27}\frac{1}{\bar{\mu}^2}|u|^3 + \bar{\mu}|x_3|^3$$

Thus,

$$\dot{V} \leq -a_1|x|^2 + a_2|x||u| + a_3|u|^3 \tag{24}$$

where $a_2 = \varepsilon + \mu$ and $a_3 = 4/27\bar{\mu}^2$. Upon completion of squares, the last inequality yields

$$\dot{V} \leq -(a_1 - \frac{a_2}{2}\kappa)|x|^2 + \frac{a_2}{2\kappa}|u|^2 + a_3|u|^3 \tag{25}$$

where κ a positive number such that $\kappa < 2a_1/a_2$. From (25) it follows that $\dot{V} < 0$ whenever $|x| > \sqrt{c_1|u|^2 + c_2|u|^3} = \rho(|u|)$ with $c_1 = a_2/\kappa(2a_1 - a_2\kappa)$ and $c_2 = 2a_3/(2a_1 - a_2\kappa)$. Now let $c_3 = \frac{1}{2}(k_2 + \varepsilon - \sqrt{(k_2-\varepsilon)^2 + 4\mu^2})$ and $c_4 = k_2 + \varepsilon + \sqrt{(k_2-\varepsilon)^2 + 4\mu^2}$ and notice that

$$\underline{\alpha}(|x|) = c_3|x|^2 \leq V(x) \leq c_4|x|^2 + \frac{1}{3}|x|^3 = \bar{\alpha}(|x|)$$

From [6, Fact 37] it follows that $\gamma_2'(s) = \underline{\alpha}^{-1}(\bar{\alpha}(\rho(s))) = \sqrt{b_1 s^2 + b_2 s^3 + (b_3 s^2 + b_4 s^3)^{3/2}}$ where $b_1 = c_4 c_1/c_3$, $b_2 = c_4 c_2/c_3$, $b_3 = c_1/(3c_3)^{2/3}$, $b_4 = c_2/(3c_3)^{2/3}$. ∎

The following corollary is immediate from Lemma 1 and the definition of y_2.

Corollary 1 *Let the system (20). Then*

$$\|y_2\|_a \leq \gamma_2(\|u\|_a) \tag{26}$$

where $\gamma_2(s) = b_1 s^2 + b_2 s^3 + (b_3 s^2 + b_4 s^3)^{3/2}$ *and* b_i *(*$i = 1, \ldots, 4$*) as in Lemma 1.*

The next result shows that a linear system with a neutrally stable state matrix can be stabilized by a saturating control. The resulting closed-loop system has a linear gain and a non-zero input restriction from the disturbance channel.

Lemma 2 ([11]) *Consider the linear system*

$$\dot{x} = Ax + Bu + d$$

Assume that the pair (A, B) is stabilizable and that the matrix A is neutrally stable, i.e., there exists a positive-definite matrix $P > 0$ such that

$$A^T P + PA \leq 0 \tag{27}$$

Then there exists $N, \Delta > 0$ such that when

$$u = -\lambda\,\mathrm{sat}(\frac{B^T P x}{\lambda}) \tag{28}$$

we have that, for each $\lambda > 0$,

$$\|d\|_a \leq \lambda\Delta \Rightarrow \|x\|_a \leq N\|d\|_a \tag{29}$$

The following result gives a control law that globally stabilizes the system (6).

Proposition 1 *Let k_2, k_3 be positive numbers such that the matrix A in (18) is neutrally stable. Let $P > 0$ be a matrix that satisfies (27). Let $\lambda > 0$ be such that*

$$b_1\lambda + b_2\lambda^2 + (b_3\lambda^{4/3} + b_4\lambda^{7/3})^{3/2} \leq \min\{\Delta, 1/NL\}$$

Then the control law

$$v = -k_2 x_2 - k_3 x_3 - \lambda\,\mathrm{sat}\left(\frac{B^T P x}{\lambda}\right) \tag{30}$$

globally asymptotically stabilizes (6).

Proof: From Corollary 1 we have that $\|d\|_a \leq \gamma_2(\|u\|_a)$ and (11) is satisfied (here $\delta_2 = 0$) for (P2). From the definition of u it follows that $|u| \leq \min\{\lambda, L|x|\}$ where $L = \max_i \sum_j |[B^T P]_{ij}|$. From (29) it then follows that $\|u\|_a \leq \min\{N\lambda, NL\|d\|_a\}$ and (10) is satisfied with $\gamma_1(s) = NLs\}$. Choose now $\lambda > 0$ such that $\gamma_1(\gamma_2(s)) < s$ for all $s \in [0, \lambda]$, i.e., $NL = \sup_{s\in[0,\lambda]} \gamma_1(\gamma_2(s))/s = NL(b_1\lambda + b_2\lambda^2 + (b_3\lambda^{4/3} + b_4\lambda^{7/3})^{3/2}) < 1$. The compatibility condition (13) is satisfied choosing $\sup_{s\in[0,\lambda]} \gamma_2(s) \leq \lambda\Delta$ or $b_1\lambda + b_2\lambda^2 + (b_3\lambda^{4/3} + b_4\lambda^{7/3})^{3/2} \leq \Delta$. The result then follows from Theorem 1[2]. ∎

[2]Notice that the input to (P2) is always bounded by λ so it is only necessary to ensure that $\gamma_2(\lambda) \leq \Delta$ in (13).

Remark 1 *The feedback control $B^T Px$ in (30) can be substituted by another feedback Fx such that the matrix $A-BF$ is Hurwitz. Such a matrix F can be found using the results of [17, 11].*

Remark 2 *From (24) one also obtains that $\dot{V} < 0$ if*

$$|x| > \frac{a_2}{2a_1}|u| + \sqrt{\frac{a_2^2}{4a_1^2}|u|^2 + \frac{a_3}{a_1}|u|^3} = \rho(|u|)$$

Using this expression, an alternative expression for the gain γ_2 results. The details are left to the reader.

6 Control with Hard Saturation

The control law (30) is only partly saturated. In case x_2 and x_3 become large, this control law may not be acceptable. An alternative, local, design can be completed by noticing that the linearization of (6) is given by

$$\begin{aligned} \dot{x}_1 &= x_2 \\ \dot{x}_2 &= \varepsilon x_3 \\ \dot{x}_3 &= v \end{aligned} \tag{31}$$

References [18, 17] provide saturating control laws for stabilizing (31).

Proposition 2 ([18]) *Consider the control law*

$$\begin{aligned} v = -\mathrm{sat}\Bigg(x_3 + \frac{1}{4}\,\mathrm{sat}\Bigg(\frac{4}{\varepsilon}x_2 + 4x_3 \\ + \frac{4}{10}\,\mathrm{sat}\left(\frac{10}{\varepsilon}x_1 + \frac{20}{\varepsilon}x_2 + 10x_3\right)\Bigg)\Bigg) \end{aligned} \tag{32}$$

Then this control law globally asymptotically stabilizes (31).

7 Numerical Example

In this section we present a numerical example of the design method presented above. We consider a rotor with $m = 14.16$ Kg, $A_g = 1531.79$ mm^2. The bias flux is taken equal to $\Phi_0 = 2.09 \times 10^{-7}$ Wb. This value is three orders of magnitude less than a typical bias flux [12] and is chosen as a challenging case of low bias operation. The nominal gap is equal to $g_0 = 0.55$ mm. The gains k_2 and k_3 are chosen to place the poles of the matrix A at $\{0, -1, -1\}$. The matrix F in Remark 1 is chosen so that the matrix $A-BF$ is Hurwitz with poles at $\{-2, -1, -1\}$. The responses for initial conditions $x_1(0) = 0.55$ mm, $x_2(0) = 0.01$ mm/sec, $x_3(0) = 0$ and for different values of λ are shown in Figs. 5-8. Figures 7 and 9 show the corresponding parts of the control inputs. There, $e_1 = -k_2x_2 - k_3x_3$ and $e_2 = -\lambda\mathrm{sat}(((F\,x)/\lambda)$. The total input is $e = e_1 + e_2$.
Next, we perform simulations with the control law (32). Figure 10 shows the trajectories of the system using this control law. The saturation level was taken equal

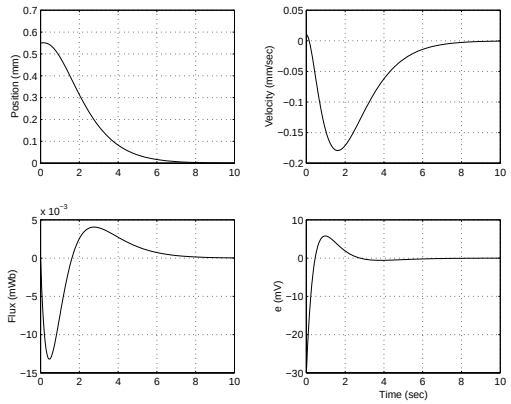

Figure 5: System trajectories and control input for $\lambda = 10^{-4}$ (40 mV).

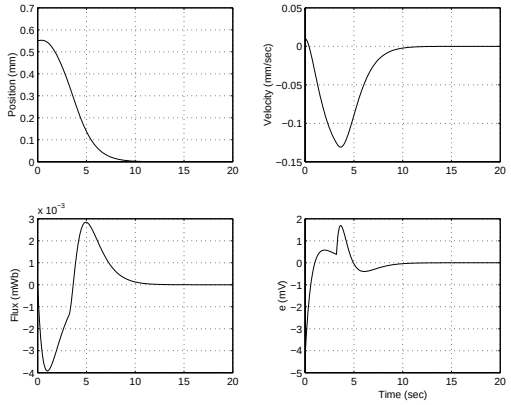

Figure 6: System trajectories and control input for $\lambda = 10^{-5}$ (4 mV).

to 0.1 Volts (100 mV). The solid lines show the trajectories for the linearized system (31) and the dashed lines show the trajectories for the original, nonlinear system (6). Notice that although the controller does not saturate, the saturation level has a strong effect on the system performance. To see this, we also performed a simulation with a very small saturation level.
To demonstrate a severe limitation on the maximum voltage, a saturation level to 5 mV was chosen. The results are shown in Fig. 11. The controller is kept to always a fraction the maximum saturation level. As expected, this is achieved at the price of slower convergence to the origin.

Acknowledgment: The authors wish to thank Prof. Andrew Teel and Dr. Murat Arcak for helpful discussions during the preparation of the final version of this paper.

References

[1] P. Allaire, M. Kasarda, and L. K. Fujita, "Rotor power losses in planar radial magnetic bearings - effects of number of stator poles, air gap thickness, and magnetic flux density," in *Proceedings of the 1998 International Gas Turbine and Aeroengine Congress and*

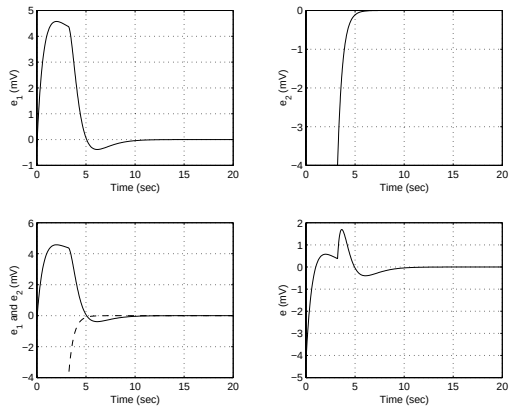

Figure 7: Control inputs for $\lambda = 10^{-5}$ (4 mV).

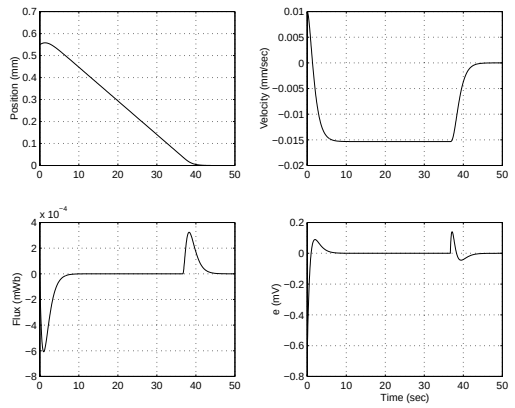

Figure 8: System trajectories and control input for $\lambda = 10^{-6}$ (0.4 mV).

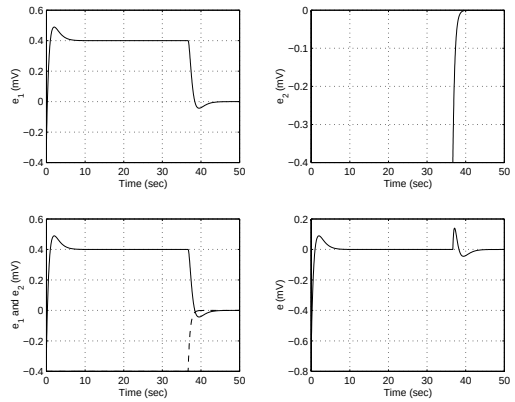

Figure 9: Control inputs for $\lambda = 10^{-6}$ (0.4 mV).

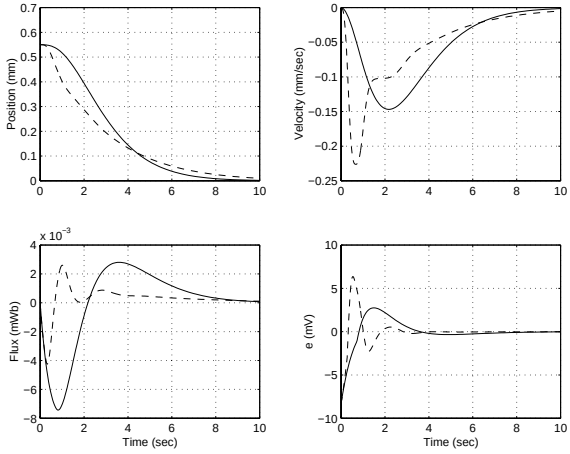

Figure 10: Simulations with maximum saturation level 100 mV.

Exhibition, 1998. Stockholm, Sweden.

[2] M. D. Anderson and S. C. Dodd, "Battery Energy Storage Technologies," *International Journal of Control*, Vol. 81, No. 3, pp. 475–479, 1993.

[3] Anonymous, "Economic and Technical Feasibility Study for Energy Storage Flywheels," December 1983. Technical Report ERDA-76-65.

[4] J. C. Anselmo, "Technology Leaps Shape Satellites of Tomorrow," *Aviation Week and Space Technology*, pp. 56–58, January 25 1999.

[5] A. Charara, J. De Miras, and B. Caron, "Nonlinear Control of a Magnetic Levitation System Without Premagetization," *IEEE Transactions on Control Systems Technology*, Vol. 4, No. 5, pp. 513–523, 1996.

[6] J. M. Coron, L. Praly, and A. Teel, "Feedback Stabilization of Nonlinear Systems: Sufficient Conditions and Lyapunov and Input-Output Techniques," in *Trends in Control: A European Perspective* (A. Isidori, ed.), pp. 293–348, London: Springer-Verlag, 1995.

[7] C. D. Hall, "High-Speed Flywheels for Integrated Energy Storage and Attitude Control," in *Proceedings of the American Control Conference*, pp. 1894–1898, 1997. Albuquerque, NM.

[8] D. Johnson, G. V. Brown, and D. J. Inman, "Adaptive Variable Bias Magnetic Bearing Control," in *American Control Conference*, (Philadelphia, PA), pp. 2217–2223, 1998.

[9] C. Knospe and C. Yang, "Gain-Scheduled Control of a Magnetic Bearing with Low Bias Flux," in *36th Conference on Decision and Control*, (San Diego, CA), pp. 418–423, 1997.

[10] M. Krstić, I. Kanellakopoulos, and P. Kokotović, *Nonlinear and Adaptive Control Design*, New York: Wiley and Sons, 1995.

[11] W. Liu, Y. Chitour, and E. Sontag, "On Finite-Gain Stabilizability of Linear Systems Subject to Input Saturation," *SIAM Journal on Control and Optimization*, Vol. 34, No. 4, pp. 1190–1219, 1996.

[12] A. Mohamed and I. Busch-Vishniac, "Imbalance Compensation and Automation Balancing in Magnetic Bearing Systems Using the Q-Parameterization Theory," *IEEE Trans. Control System Technology*, Vol. 3, No. 2, pp. 202–211, 1995.

[13] P. Proctor, "Flywheels Show Promise for 'High-Pulse' Satellites," *Aviation Week and Space Technology*, p. 67, January 25 1999.

[14] N. N. Rao, *Elements of Engineering Electromagnetics*, Englewood Cliffs, NJ: Prentice Hall, 4th ed., 1994.

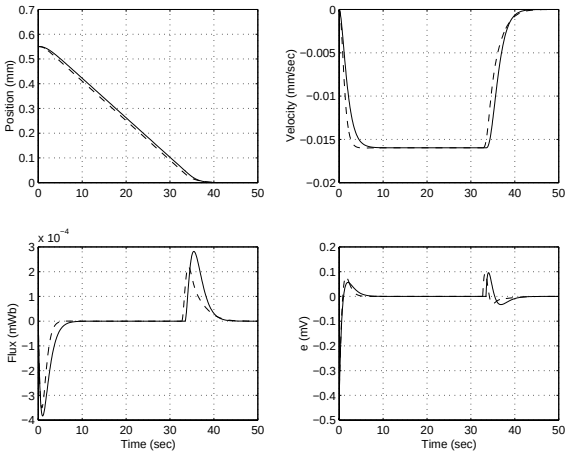

Figure 11: Simulations with maximum saturation level 5 mV.

[15] G. E. Rodriguez, P. A. Studer, and D. A. Baer, "Assessment of Flywheel Energy Storage for Spacecraft Power Systems," 1983. Technical Report TM-85061.

[16] J. R. Stuart and J. G. Stuart, "Revolutionary Next Generation Satellite Communications Architectures and Systems," in *Proceedings of the 1997 IEEE Aerospace Conference*, pp. 535–545, 1997. Aspen, CO.

[17] H. Sussmann, E. D. Sontag, and Y. Yang, "A General Result on the Stabilization of Linear Systems Using Bounded Controls," *IEEE Transactions on Automatic Control*, Vol. 39, No. 12, pp. 2411–2425, 1994.

[18] A. Teel, "Global Stabilization and Restricted Tracking for Multiple Integrators with Bounded Controls," *Systems and Control Letters*, Vol. 18, pp. 165–171, 1992.

[19] A. Teel, "A Nonlinear Small Gain Theorem for the Analysis of Control Systems with Saturation," *IEEE Transactions on Automatic Control*, Vol. 41, No. 9, pp. 1256–1270, 1996.